Crystal Structures

International Edition: DOI: 10.1002/anie.201709240
German Edition: DOI: 10.1002/ange.201709240

A High-Resolution Crystal Structure that Reveals Molecular Details of Target Recognition by the Calcium-Dependent Lipopeptide Antibiotic Laspartomycin C

Laurens H. J. Kleijn[+], Hedwich C. Vlieg[+], Thomas M. Wood, Javier Sastre Toraño, Bert J. C. Janssen, and Nathaniel I. Martin**

Abstract: *The calcium-dependent antibiotics (CDAs) are an important emerging class of antibiotics. The crystal structure of the CDA laspartomycin C in complex with calcium and the ligand geranyl-phosphate at a resolution of 1.28 Å is reported. This is the first crystal structure of a CDA bound to its bacterial target. The structure is also the first to be reported for an antibiotic that binds the essential bacterial phospholipid undecaprenyl phosphate (C_{55}-P). These structural insights are of great value in the design of antibiotics capable of exploiting this unique bacterial target.*

Key to addressing the growing threat of drug-resistant bacteria is the identification and characterization of antibiotics that operate by unexploited mechanisms.[1,2] Notable in this regard are the calcium-dependent antibiotics (CDAs), which have gained clinical prominence owing to their activity against multi-drug-resistant pathogens.[3–5] While a variety of antibacterial mechanisms have been ascribed to the various CDAs, an atomic-level understanding of the recognition of their bacterial target(s) remains elusive. At present, daptomycin is the only clinically used CDA, and its mode of action is the topic of ongoing investigation.[6–9] By comparison, the structurally similar CDAs laspartomycin C, friulimycin B, tsushimycin, and amphomycin have more clearly understood antibacterial mechanisms.[10–14] It was recently reported that laspartomycin C forms a high-affinity complex ($K_d = 7.3 \pm 3.8$ nM) with the bacterial cell wall precursor undecaprenyl phosphate (C_{55}-P) and in doing so inhibits peptidoglycan biosynthesis, ultimately leading to cell death.[14] Notably, the sequestration of C_{55}-P is a mechanism not exploited by any current clinically used antibiotic making it an attractive target for further study. To date, the only structural insights available for the C_{55}-P binding CDAs are provided by the unliganded structure of tsushimycin.[15] To achieve a deeper understanding of the high-affinity C_{55}-P binding and specificity, herein we report the crystal structure of laspartomycin C in complex with calcium and geranyl phosphate (C_{10}-P, a soluble C_{55}-P analogue) at a resolution of 1.28 Å. The target specificity of laspartomycin C was also studied by examining its interaction with other common phospholipids. Furthermore, the stereochemical implications of laspartomcyin C target binding revealed by the crystal structure were probed by synthesizing and testing the enantiomeric form of the antibiotic. Not only is the structure here reported the first for a CDA in complex with both calcium and its biomolecular target, it is also the first for any antibiotic that targets C_{55}-P.

While laspartomycin C can be isolated from fermentation of *S. viridochromogenes*,[16,17] it was found to be more convenient to prepare the compound by synthetic means as previously described (see the Supporting Information for synthetic details).[14] The calcium-dependent antibiotic activity of the synthetic laspartomycin C was confirmed against a number of bacterial strains, including drug-resistant pathogens (Supporting Information, Table S1). Crystals of the laspartomycin C/Ca^{2+}/geranyl phosphate (C_{10}-P) complex were grown and diffracted to 1.28 Å resolution (Supporting Information, Table S3). The refined structure reveals a stoichiometry for the complex of a single laspartomycin C molecule bound to one geranyl phosphate ligand along with two calcium ions playing key roles in mediating recognition (Figure 1).

Laspartomycin C adopts a saddle-shaped amphipathic fold with polar residues (Asp^5, Asp^7, D-*allo*-Thr^9) aligning the top plain and aliphatic residues (D-Pip^3 and Pro^{11}) forming the hydrophobic bottom plane from which the fatty acid side chain protrudes downwards (Figure 2). The cavity created within the laspartomycin C macrocycle envelops the phosphate head group of the C_{10}-P, which is held in place by hydrogen bonding to the peptide backbone and chelation of both calcium ions. The C_{10}-P isoprenyl tail appears to be stabilized by hydrophobic interactions with the laspartomycin C fatty acid side chain as it exits the binding pocket. The complex is well-resolved except for the outermost parts of the C_{10}-P isoprenyl tail and the laspartomycin C fatty acid side

[*] L. H. J. Kleijn,[+] T. M. Wood, J. Sastre Toraño, Dr. N. I. Martin
Department of Chemical Biology & Drug Discovery, Utrecht Institute for Pharmaceutical Sciences, Utrecht University
Universiteitsweg 99, 3584 CG Utrecht (The Netherlands)
E-mail: n.i.martin@uu.nl
H. C. Vlieg,[+] B. J. C. Janssen
Crystal and Structural Chemistry, Bijvoet Center for Biomolecular Research, Utrecht University
Padualaan 8, 3584 CH Utrecht (The Netherlands)
E-mail: b.j.c.janssen@uu.nl
[+] These authors contributed equally to this work.
Supporting information and the ORCID identification number(s) for the author(s) of this article can be found under: https://doi.org/10.1002/anie.201709240.

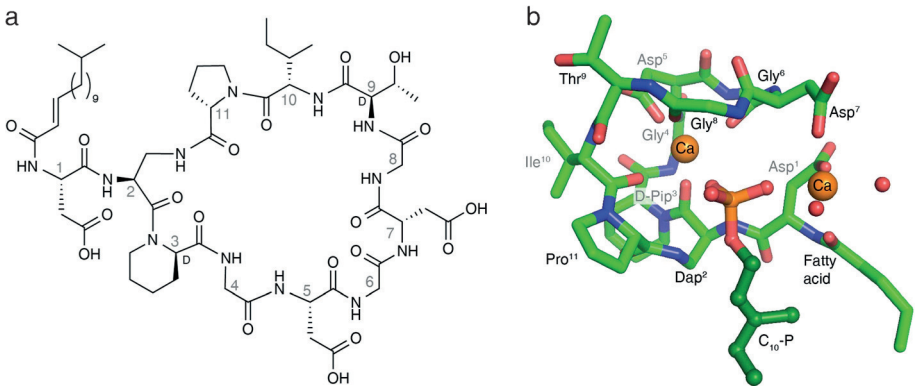

Figure 1. Laspartomycin C forms a 1:1:2 complex with C_{10}-P and Ca^{2+}. a) Structure of laspartomycin C. b) Structure of the ternary complex with laspartomycin C (green stick representation), two bound Ca^{2+} ions (orange spheres), bound water molecules (red spheres), and the C_{10}-P ligand (dark green ball-and-stick representation). The Ca^{2+} ion on the left is referred to as the central Ca^{2+} ion and the Ca^{2+} ion on the right as the peripheral Ca^{2+} ion.

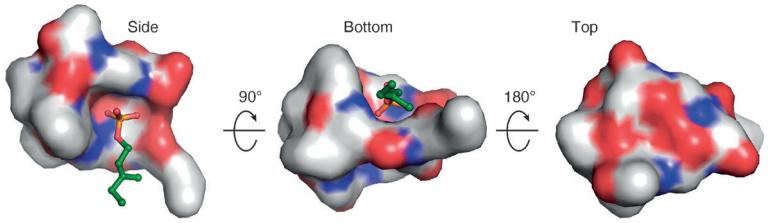

Figure 2. Surface distribution of polar regions of the Laspartomycin C/Ca^{2+}/C_{10}-P complex. The "top" and the sides of the complex are hydrophilic whereas the bottom face is much more hydrophobic. The C_{10}-P ligand (green) is bound within the cavity of the laspartomycin C macrocycle. The atoms in laspartomycin C are colored as follows: O red, N blue, C white.

chain. In the crystal lattice, the C_{10}-P isoprenyl units and fatty acid side chains of multiple complexes cluster together to form continuous hydrophobic sheets (Supporting Information, Figure S13). This may also hint at the biologically relevant orientation that laspartomycin C adopts on the bacterial cell surface in its sequestration of C_{55}-P at the membrane interface.

The structure of the complex provides an explanation for the high-affinity binding of C_{55}-P by laspartomycin C. Target recognition takes place via direct interactions of the phospholipid head group with the laspartomycin C backbone and both calcium ions (Figure 3). The backbone and side chain amides of Dap^2 as well as the backbone amide of Gly^8 form hydrogen bonds with three of the four phosphate oxygen atoms (Supporting Information, Table S4). Of key importance are the two calcium ions that interact with the phosphate moiety as part of an octahedral coordination symmetry. The central Ca^{2+} is coordinated by 5 interactions with laspartomycin C involving four backbone carbonyls (Dap^2, Gly^6, Gly^8, Ile^{10}) and one aspartic acid side chain (Asp^5) with all distances (2.3 Å) in agreement with expected Ca–O coordination distances (Figure 3b; Supporting Information, Table S5).[18] The peripheral Ca^{2+} is bound via interactions provided by two aspartic acid side chains (Asp^1, Asp^7) and the N-terminal fatty acid carbonyl group along with two H_2O molecules that complete the octahedral coordination (Figure 3c).

The binding of C_{10}-P by laspartomycin C as revealed by the crystal structure is not intrinsically dependent on a chiral interaction. To confirm this, we synthesized the enantiomeric form of laspartomycin C. As expected, circular dichroism (CD) analysis of laspartomycin C and its enantiomer yielded identical ellipticities of opposite sign with clear effects observed in the absence and presence of Ca^{2+} (Supporting Information, Figures S5,S6). Additionally, the CD spectra of both peptides indicate a second significant conformational change upon addition of 1.0 equiv of C_{10}-P. Addition of excess C_{10}-P did not result in further elliptic changes, in line with a 1:1 peptide:C_{10}-P binding stoichiometry. Finally, antibiotic testing of *ent*-laspartomycin C in parallel with laspartomycin C showed identical antibiotic minimum inhibitory concentrations (MICs) for both compounds against a panel of five Gram-positive pathogens (Supporting Information, Table S1).

The specificity of laspartomycin C binding to phosphate monoesters was evaluated using an antagonization assay wherein the antibiotic peptide was pre-mixed with various phospholipids and the effect on activity assessed (Figure 3d; Supporting Information, Figure S7–S9). Mixing laspartomycin C with inorganic phosphate (HPO_4^{2-}) at concentrations corresponding to normal serum levels resulted in no observable antagonization. As expected, treatment of laspartomycin C with 1.0 equivalent of C_{10}-P led to loss of antibiotic activity while the activity of daptomycin was not inhibited by C_{10}-P addition even at higher concentrations. We also assessed the antagonization potential of a C6 truncated variant of the aliphatic mammalian lipid phosphatidic acid (C_6-PA). These studies revealed that C_6-PA is also capable of blocking the antibiotic action of laspartomycin C, with 1.0 mol equiv eliciting complete antagonization. This effect appears to be specific for phosphate monoesters. When the common lipid phosphodiester phosphatidyl glycerol (PG) was added to laspartomycin C in equimolar amount, no antagonization was observed. In fact only after adding a large excess of PG (8.0 molar equivalents) was the activity of laspartomycin C diminished. By comparison, the activity of daptomycin is much more readily antagonized by PG with 2.0 mol equiv, leading to complete loss of antibiotic action. Interestingly, PG is found in high concentrations in mammalian lung surfactant and is the likely cause of the ineffectiveness of daptomycin in treating lung infections.[19] The effect of various biologically relevant phosphate monoesters on the activity of laspartomycin C was also investigated. No appreciable antagonization of activity was observed when laspartomycin C was treated

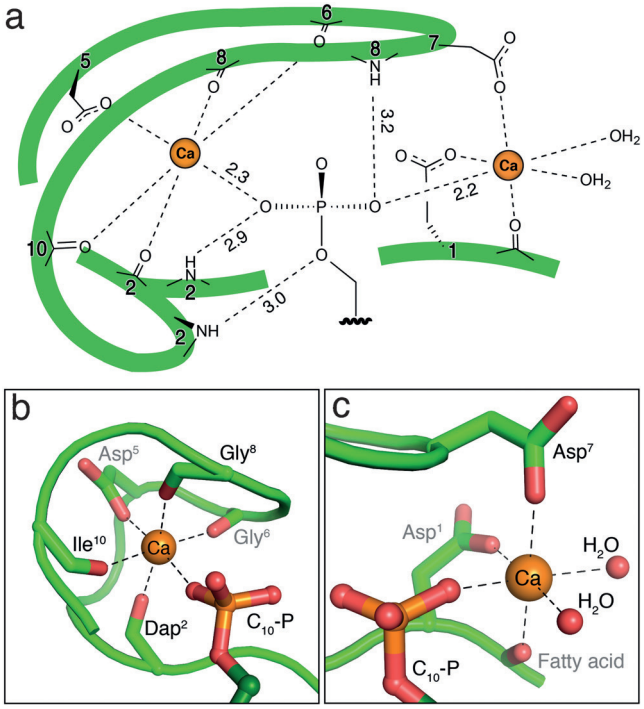

d

Compound	Na_2HPO_4	C_{10}-P	C_6-PA	PG
Laspartomycin C	-	+	+	-
Daptomycin	-	-	-	+

Figure 3. Target recognition by laspartomycin C. a) The C_{10}-P phosphate headgroup interacts via the coordinated Ca^{2+} ions and three laspartomycin C backbone amides. b) The central Ca^{2+} ion is coordinated by backbone carbonyl and side chain interactions as well as the C_{10}-P head group. c) The peripheral Ca^{2+} ion is coordinated by two side chain interactions, the fatty acid carbonyl, and the C_{10}-P head group with octahedral coordination completed by two water molecules. d) Antagonization of the antibiotic activity of laspartomycin C and daptomycin. Antibiotic activity was antagonized (+) or unaffected (−) by the presence of $\leq$2.0 mol equiv antagonist. Antagonization by Na_2HPO_4 was assessed employing a fixed 1.25 mM concentration corresponding to 24 and 500 mol equiv for laspartomycin C and daptomycin, respectively. Full data given in the Supporting Information, Table S2 and Figures S7–S9.

with adenosine 5′-monophosphate, *rac*-glycerol-1-phosphate, dihydroxyacetone phosphate, glucose 6-phosphate, *O*-phospho-L-serine, or γ,γ-dimethylallyl phosphate (Supporting Information, Table S2). Furthermore, to examine the role played by the length of the alkyl substituent, a series of saturated linear C1, C3, C6, and C10 phosphate monoesters where prepared and tested for their ability to impact the activity of laspartomycin C. These investigations revealed that only the C10 saturated linear phospholipid caused antagonization, suggesting that shorter unbranched aliphatic lipid tails do not support high affinity phosphate monoester binding by laspartomycin C.

The laspartomycin C crystal structure provides key insights into the structural feature that differentiate the antibiotic mechanisms of the lipopeptide and lipodepsipeptide CDA subclasses. In the case of laspartomycin C the side chain of Dap^2 closes the peptide macrocycle via an amide bond with the C-terminal proline. This newly formed amide linkage plays a role in target recognition as it contributes a hydrogen bonding interaction with the phosphate group in the binding pocket (Figure 3a). Conversely, for lipodepsipeptide CDAs such as daptomycin an ester linkage is found at this position, resulting from cyclization of the C-terminus with a threonine side chain. The ester linkage found in daptomycin is unable to serve as a H-bond donor and instead a repulsive electrostatic oxygen-oxygen interaction is expected to arise when encountering a phosphate monoester.

The laspartomycin C/Ca^{2+}/C_{10}-P ternary complex exists as a dimer in the asymmetric unit related by a two-fold rotation and is stabilized by direct and indirect interactions between the two ternary units (Figure 4). We also found evidence for the formation of the dimeric species in solution based on mass spectrometry studies (Supporting Information, Figures S10–S12). The two ternary units in the dimer are nearly identical to each other with only a substantial difference in the side chain rotamer for D-*allo*-Thr^9 (Supporting Information, Figure S14). As illustrated in Figure 4, there are a number of interactions unique to the dimer. A hydrogen bond is observed between the D-*allo*-Thr^9 backbone amide of one laspartomycin C molecule and the Asp^7 side chain carboxylate of the other. Additional indirect hydrogen bonding interactions are mediated by the D-*allo*-Thr^9 backbone carbonyl with the water molecules coordinated by the peripheral Ca^{2+} of the other ternary unit (Supporting Information, Figure S15). The fatty acid side chain of one laspartomycin C molecule has hydrophobic interactions with the Pro^{11} side chain of the other molecule in the dimer. Furthermore, the absence of a sidechain in Gly^8 prevents steric hindrance from occurring at the dimer interface.

In the dimer complex, the two C_{10}-P phosphate head groups are fully coordinated and completely sequestered from the solvent. The two C_{10}-P head groups also directly interact through a hydrogen bond (Figure 4; Supporting Information, Table S6). Furthermore, the isoprenyl tails of the two C_{10}-P ligands have hydrophobic interactions with each other and with the Pro^{11} side chains in the opposing laspartomycin C monomers. The more distal part of the isoprenyl tails are not stabilized in the complex and disor-

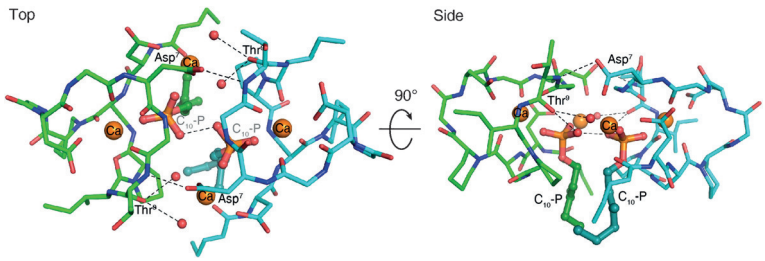

Figure 4. The laspartomycin C/Ca^{2+}/C_{10}-P complex is a dimer in the crystal. Two views of the dimer interface, with cross-dimer interactions shown as dotted lines. The two laspartomycin C chains of the two ternary complexes that make up the dimer are colored green and cyan. For clarity, in the side view only the interactors closest to the viewer are labeled.

dered in the crystals. The full coordination of the C_{10}-P headgroup and the interactions of laspartomycin C with the headgroup-proximal part of the isoprenyl tails in the dimer complex is consistent with the high-affinity laspartomycin C-undecaprenyl phosphate interaction and explains the specificity of laspartomycin C for phosphate monoesters with both long and short hydrocarbon tails.

A straightforward model of how laspartomycin C is positioned on the bacterial membrane follows from the C_{10}-P bound dimer structure. The two laspartomycin C fatty acid side chains and the two C_{10}-P isoprenyl tails are all orientated perpendicular to a hydrophobic plane formed by the bottom sides of two laspartomycin C molecules in the dimer (Supporting Information, Figure S16). This plane is likely oriented parallel to the cell surface. The C_{10}-P head groups are sequestered above the hydrophobic bottom plane within the core of the laspartomycin C dimer. This suggests that when bound to C_{55}-P, laspartomycin C is slightly embedded in the bacterial membrane and that the hydrophobic side chains of D-Pip^3 and Pro^{11} contribute to interactions with the hydrophobic part of the lipid bilayer. Structural features that are important for dimer formation and Ca^{2+} binding are predominantly conserved within the CDA family. Notably, the structure of the unliganded tsushimycin/Ca^{2+} complex is also dimeric[15] and superimposes closely to our laspartomycin C dimer in complex with Ca^{2+} and C_{10}-P (Supporting Information, Table S7, Figure S17). Whether this indicates that the structures of all CDAs are similar and whether they all form dimers awaits further experimental verification.

In summary, the laspartomycin C structure reported herein is the first of a CDA bound to its bacterial target and provides a clear explanation for the two conserved calcium-binding sites common to all CDAs. Furthermore, it is also is the first structure to be reported for an antibiotic that binds the essential bacterial phospholipid C_{55}-P. At present, no clinically used antibiotics operate via C_{55}-P binding. Our findings provide a structural blueprint for the design of new antibiotics capable of exploiting this unique bacterial target.

Acknowledgements

We thank Johan Kemmink for assistance in recording 2D NMR spectra. Financial support provided by Utrecht University and the Netherlands Organization for Scientific Research (NWO) is acknowledged. L.H.J.K. and T.M.W. were supported by NWO PhD student grants, H.C.V. by NWO grant no 01.80.104.00, B.J.C.J. by NWO-VIDI grant no 723.012.002, and N.I.M. by an NWO-VIDI grant no. 016.102.338.

Conflict of interest

The authors declare no conflict of interest.

Keywords: bacterial cell wall · C_{55}-P · calcium-dependent antibiotics · crystal structure · laspartomycin c

How to cite: *Angew. Chem. Int. Ed.* **2017**, *56*, 16546–16549
Angew. Chem. **2017**, *129*, 16773–16776

[1] M. F. Chellat, L. Raguz, R. Riedl, *Angew. Chem. Int. Ed.* **2016**, *55*, 6600–6626; *Angew. Chem.* **2016**, *128*, 6710–6738.
[2] R. Tommasi, D. G. Brown, G. K. Walkup, J. I. Manchester, A. A. Miller, *Nat. Rev. Drug Discovery* **2015**, *14*, 529–542.
[3] T. Schneider, A. Mullera, H. Miess, H. Gross, *Int. J. Med. Microbiol.* **2014**, *304*, 37–43.
[4] M. Strieker, M. A. Marahiel, *ChemBioChem* **2009**, *10*, 607–616.
[5] Book chapter "*The Cyclic Lipopeptide Antibiotics*": L. H. J. Kleijn, N. I. Martin, *Topics in Medicinal Chemistry*, *Vol. 47*, Springer, Berlin, **2017**, pp. 1–27. https://doi.org/10.1007/7355_2017_9.
[6] J. Zhang, W. R. P. Scott, F. Gabel, M. Wu, R. Desmond, J. Bae, G. Zaccai, W. Russ Algar, S. K. Straus, *Biochim. Biophys. Acta* **2017**, *1865*, 1490–1499.
[7] S. D. Taylor, M. Palmer, *Bioorg. Med. Chem.* **2016**, *24*, 6253–6268.
[8] A. Muller, M. Wenzel, H. Strahl, F. Grein, T. N. Saaki, B. Kohl, T. Siersma, J. E. Bandow, H. G. Sahl, T. Schneider, L. W. Hamoen, *Proc. Natl. Acad. Sci. USA* **2016**, *113*, E7077–E7086.
[9] J. Pogliano, N. Pogliano, J. A. Silverman, *J. Bacteriol.* **2012**, *194*, 4494–4504.
[10] T. Schneider, K. Gries, M. Josten, I. Wiedemann, S. Pelzer, H. Labischinski, H. G. Sahl, *Antimicrob. Agents Chemother.* **2009**, *53*, 1610–1618.
[11] E. Rubinchik, T. Schneider, M. Elliott, W. R. Scott, J. Pan, C. Anklin, H. Yang, D. Dugourd, A. Muller, K. Gries, S. K. Straus, H. G. Sahl, R. E. Hancock, *Antimicrob. Agents Chemother.* **2011**, *55*, 2743–2754.
[12] D. Dugourd, H. Yang, M. Elliott, R. Siu, J. J. Clement, S. K. Straus, R. E. Hancock, E. Rubinchik, *Antimicrob. Agents Chemother.* **2011**, *55*, 3720–3728.
[13] P. 't Hart, L. H. J. Kleijn, G. de Bruin, S. F. Oppedijk, J. Kemmink, N. I. Martin, *Org. Biomol. Chem.* **2014**, *12*, 913–918.
[14] L. H. J. Kleijn, S. F. Oppedijk, P. 't Hart, R. M. van Harten, L. A. Martin-Visscher, J. Kemmink, E. Breukink, N. I. Martin, *J. Med. Chem.* **2016**, *59*, 3569–3574.
[15] G. Bunkóczi, L. Vertesy, G. M. Sheldrick, *Acta Crystallogr. Sect. D* **2005**, *61*, 1160–1164.
[16] H. Naganawa, M. Hamada, K. Maeda, Y. Okami, T. Takeushi, *J. Antibiot.* **1968**, *21*, 55–62.
[17] D. B. Borders, R. A. Leese, H. Jarolmen, N. D. Francis, A. A. Fantini, T. Falla, J. C. Fiddes, A. Aumelas, *J. Nat. Prod.* **2007**, *70*, 443–446.
[18] M. M. Harding, *Acta Crystallogr. Sect. D* **2006**, *62*, 678–682.
[19] J. A. Silverman, L. I. Mortin, A. D. Vanpraagh, T. Li, J. Alder, *J. Infect. Dis.* **2005**, *191*, 2149–2152.

Manuscript received: September 6, 2017
Revised manuscript received: October 21, 2017
Accepted manuscript online: November 6, 2017
Version of record online: November 30, 2017

